

# Metrology-Design Co-Optimization for BEOL Dimensional Characterization using Scatterometry

Stefan Schoeche\*<sup>a</sup>, Daniel Schmidt<sup>a</sup>, Pádraig Timoney<sup>a</sup>, Aron Cepler<sup>b</sup>, Marjorie Cheng<sup>b</sup>, and Igor Turovets<sup>c</sup>

<sup>a</sup>IBM Research, 257 Fuller Road, Albany, NY 12203, USA

<sup>b</sup>Nova Measuring Instruments Inc., 3342 Gateway Blvd, Fremont, CA 94538, USA

<sup>c</sup>Nova Ltd., 5 David Fikes St., Rehovot, 7632805, Israel

## ABSTRACT

A systematic study of the co-optimization of target design and metrology technique is presented to accurately measure the critical dimensions of backend of line (BEOL) metal line gratings. Rigorous coupled-wave analysis calculations and machine learning approaches are combined to evaluate various design scenarios with and without patterned underlayers in conjunction with either traditional scatterometry or vertical traveling scatterometry (VTS) using spectral interferometry. It was found that for traditional scatterometry techniques employing polarized reflectometry or ellipsometry, two levels of crossed metal lines buried below the level of interest are often sufficient to suppress most of the optical contributions from any underlayer stack beneath. Alternatively, VTS utilizing spectral interferometry and signal filtering can suppress all contributions from the underlayer stack independent of the design choice thus only the top layer of interest needs to be considered in the model analysis. Machine learning models trained on VTS data instead of traditional scatterometry data can improve the accuracy and ease of setup, for example, by utilizing simplified targets for training. Three relevant BEOL cases for measurements after an etch step, a polishing step, and dielectric layer deposition on patterned metal lines are addressed.

**Keywords:** Scatterometry, OCD, BEOL Metrology, Spectral Interferometry, Metrology

\*Corresponding author: [sschoeche@ibm.com](mailto:sschoeche@ibm.com)

## 1. INTRODUCTION

Scatterometry, or optical critical dimension (OCD) metrology, is commonly applied to non-destructively monitor the geometry of three-dimensional features during semiconductor manufacturing [1,2]. Dedicated metrology targets in the scribe line may be designed to mimic the fully integrated process flow or simplified targets might focus on specific mask levels while preventing processing or promoting complete removal of prior levels. In the backend of line (BEOL), for example, line-space gratings can be utilized to monitor critical dimensions (CD) of the metal lines that form the interconnects as well as layer thicknesses [3]. However, especially with wafer front-side and back-side processing, many different pitches and dimensions will be present throughout the stack [4]. Complicated underlayer stacks (i.e. front-end-of-line (FEOL) or mid-of-line (MOL) content when measuring from the front side or the entire front side content when measuring from the backside) can make geometrical models very challenging if not infeasible. Dedicated targets with patterning restricted to the level of interest may be a convenient solution due to the simple optical model and fast time to solution. However, besides the need to allocate valuable area within a chip for these additional targets, especially higher metal levels can present a challenge during modeling due to strong thickness interference oscillations in the presence of several hundreds of nanometers of transparent dielectric underlayer stacks. These interference oscillations might drown small spectral variations caused by subtle changes in the structured top layer of interest. Optimized target design and/or the choice of OCD measurement technique can significantly simplify this metrology challenge.

Several options to help solve these BEOL scatterometry challenges are commercially available. Machine learning (ML) is commonly applied to extract key parameters by training a model with measured spectral data and respective reference information [5]. A large data set of appropriate reference data that captures all possible stack variations is required, but it is not always easy to obtain. Differential modeling where measurement data is acquired and analyzed before and after, for example, an etch step, requires two measurements and appropriate algorithms, but does not necessarily simplify the solution [6]. One possible path is a design-optimized metrology target where the optical response can be engineered to simplify the data analysis. The best design will depend on the materials and CDs of the features studied. Any patterned

metal lines will likely need to be considered in the optical model. Phase sensitive measurements such as vertical traveling scatterometry (VTS) can be applied to filter out data content from layers below the levels of interest [7,8]. In most situations, any layers beneath the top layer are irrelevant, i.e., ideally, all spectral information below the layer of interest would be ignored.

This paper explores optimum choices for BEOL target designs to suppress unnecessary contributions from underlayer stacks and suggests scatterometry techniques that provide accurate results while simplifying the analysis and reducing turnaround times. Methodologies to quantify how well a given design suppresses underlayer contributions are derived, and three relevant case studies for measurement after a reactive ion etching (RIE) step, after a chemical mechanical polishing (CMP) step, and for determination of the interlayer dielectric (ILD) height above patterned metal lines are discussed.

## 2. EXPERIMENTAL DETAILS

We employ the Nova Prism tool which combines spectral reflectometry data with spectral interferometry capabilities. From the spectral interferometry data, absolute phase signals can be extracted to complement the polarized reflectometry data and enhance sensitivity of the tool for OCD applications [9]. In combination with appropriate algorithms, access to the absolute phase information further enables some unique capabilities absent in alternative OCD tools [7,10]. VTS utilizes filtering of the phase data to remove contributions from a complicated multilayer stack or patterned layers. This simplifies the analysis to only the geometry of interest at the top of the sample [7]. This approach helps to overcome geometrical complexities and allows focusing on the parameters of interest. Here, we explore how well this approach works for lower metal levels in the BEOL. Rigorous coupled wave analysis (RCWA) is employed for simulation and analysis of spectral reflectometry and interferometry data [11].

Various 300 mm Si short-loop wafers without FEOL/MOL content are used in the cases discussed here. Dedicated metrology targets in the scribe lines with a size of  $50 \times 50 \mu\text{m}^2$  were designed to contain blanket layers or patterned Cu line-space gratings in the levels beneath the layers of interest. EUV single or double patterning and immersion lithography were applied to pattern the features on these wafers. The conclusions generally apply to more complex wafers with FEOL/MOL or backside patterning where the benefits of the different approaches will be most relevant.

## 3. BEOL TARGET DESIGN OPTIONS

In the most straightforward approach to suppress underlayer contributions, thick opaque metal blanket pads would be placed under the level of interest. However, blanket metal pads are typically not desired in a full process flow due to dishing and defectivity concerns. Furthermore, leading edge technology nodes comprise metal levels with line heights that would result in partially transparent metal films thereby limiting the underlayer suppression capabilities of a single metal pad and rather complicate than alleviate the analysis concern discussed in this paper. This leaves four options that might be applied for the design of BEOL scatterometry targets (Fig. 1).

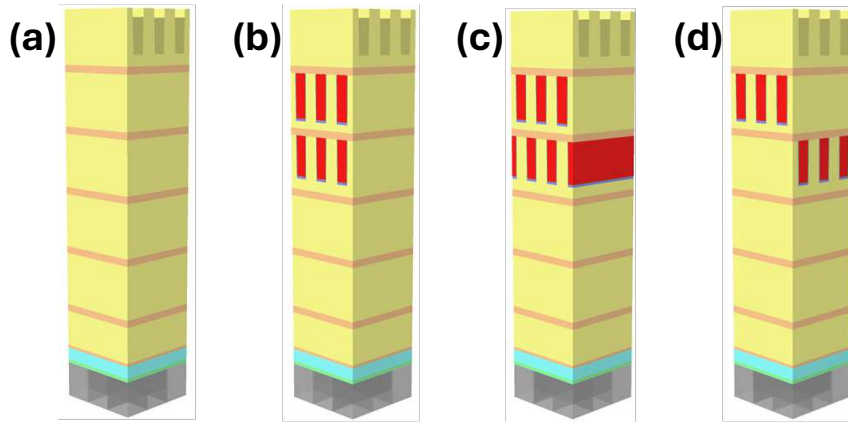


Figure 1. BEOL target design options: (a) patterning above blanket layers, (b) patterning above parallel metal lines, (c) patterning above parallel metal lines with offset, and (d) patterning above crossed metal lines.

The first option employs patterning above blanket dielectric levels, i.e., without any metal patterning underneath the level of interest. In this case, only transparent underlayers are present beneath the level of interest. While this may seem like the simplest case for optical modeling, thickness interference oscillations will be present in standard spectral reflectometry or ellipsometry data leading to parameter correlation especially for tall stacks [7]. In case of a fully-integrated wafer, all FEOL/MOL and BEOL levels would need to be included in an optical model. The second option employs patterning above parallel metal lines. A polarization-dependent blockage of the underlayer contributions can be expected in this case, i.e. for some polarization states and sample orientations all FEOL/MOL and BEOL levels need to be included in an optical model, and thickness interference oscillations and thus parameter correlation might need to be considered. The third option also utilizes patterning above parallel metal lines, but with a half-pitch offset between the metal lines. This case is intended to “close the gaps” because when viewing the structure from above it appears to mimic a blanket film. However, this situation is expected to be mainly identical to case 2 when considering electromagnetic waves. The fourth case employs patterning above crossed metal lines. A complete suppression of the underlayer stack contributions may be expected. The crossed lines must be included in the optical model, but any underlayers can be ignored if this approach is applied successfully. The effectiveness of a single pair of crossed metal lines to suppress all underlayer contributions needs to be explored. Note, option 4 may often be an obvious choice in production environments where metal levels patterned at or close to the lithographic resolution limit alternate between horizontal and vertical alignment on the wafer as preferred orientation. Also, available space for dedicated single or multi-level targets might be limited.

#### 4. RESULTS AND DISCUSSION

Figure 2 compares raw data simulations for a post-RIE step at the 6th metal level. Polarized spectral reflectivity data for two polarizations, parallel and perpendicular to the RIE trenches, were simulated for dielectric blankets only, parallel metal lines with half-pitch offset between the lines, and crossed metal lines underneath the level of interest. A half-pitch of 40 nm is considered for all patterned features.

For the dielectric blanket pad case, interference oscillations will reduce sensitivity to the level of interest parameters due to parameter correlation and much more substantial spectral signal changes caused by underlayer stack variations than variability of the RIE trench dimensions. This effect intensifies with increasing total stack height. For the parallel lines case, interference oscillations are suppressed at shorter wavelengths, but polarization perpendicular to the metal lines is not efficiently attenuated at longer wavelengths. Only the design scenario with two levels of crossed lines attenuates the optical signal from the buried dielectrics for both polarizations. The metal lines under the RIE level behave like wire-grid polarizers that only suppress the underlayer signal for all polarizations when crossed.

To quantify how efficiently specific designs suppress the underlayer contributions, different methodologies were derived and tested on relevant cases for BEOL characterization. Target design choices in combination with optimized measurement and analysis techniques are described considering accuracy, ease of setup, and time-to-solution for a RIE case, CMP case, and ILD measurement above patterned metal lines in the sections below.

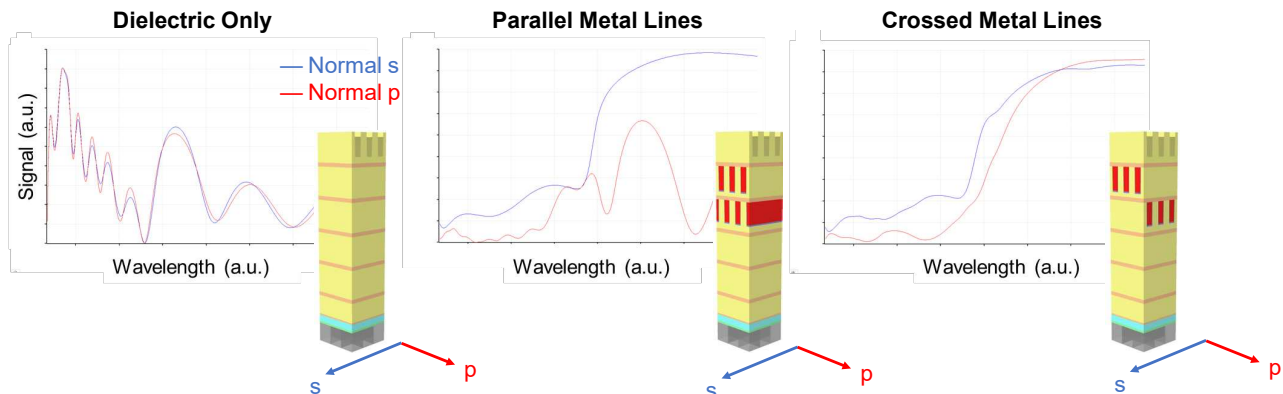


Figure 2. Simulated polarized spectral reflectivity data for a post-RIE step at the 6<sup>th</sup> metal level with dielectric blankets only, parallel metal lines and half-pitch offset between the two levels, and crossed metal lines under the level of interest. Incoming and reflected polarizations perpendicular (s) and parallel (p) to the RIE trenches at normal incidence are shown. Half-pitches of 40 nm are assumed for all patterned features.

### 4.1 Simulations for a RIE measurement at a 6<sup>th</sup> metal level

The strong interference oscillations in tall stacks of dielectric layers provide a handle to judge if a target design can successfully suppress underlayer contributions. Here, simulations for a post-RIE measurement at a 6<sup>th</sup> metal level are considered to compare the effectiveness of the four design choices outlined above. An extensive set of 1000 randomized test spectra (variability data) was created by varying all model parameters of up to 10% for the 1<sup>st</sup>, 2<sup>nd</sup>, 3<sup>rd</sup>, and 6<sup>th</sup> level while keeping the parameters of the 4<sup>th</sup> and 5<sup>th</sup> “blocking levels” fixed at nominal dimensions. Machine learning (ML) models were then trained on simulated spectral data and only the 6<sup>th</sup> level parameters were varied while keeping all other levels at nominal values.

In one test scenario, a conventional ML model was trained on polarized reflectivity data. When applying this ML model to the randomized variability data, best performance would be expected only when the underlayer contributions are suppressed. If the underlayer signal contributes to the spectral data, the ML model performance should deteriorate since that variability was not part of the training. In a second scenario, the ML model is trained on VTS data. Similarly to the first case, the model is trained on data for which only the 6<sup>th</sup> metal level parameters were varied while all other parameters were kept at nominal values. Full stack data without filtering was used for the training. For testing, an optimized filter cut-off position was determined based on data variability when plotting all training data sets together to only emphasize the contribution of the level of interest at the top. Again, when applied to the variability data set, good performance is expected only if all underlayer contributions are filtered out successfully.

Figure 3 highlights several parameters of interest for a post-RIE measurement, RIE trench height, ILD height, and trench CD, and shows a representative data set produced when applying the ML models to the variability data. Each data point represents the match of the ML model to a full spectral data set. Reported results by the ML model are shown in dependence of the known value for each simulated data set. If the underlayer contribution is successfully suppressed, the ML model trained with fixed underlayer stack should be able to match the variability data perfectly as no other source of variability contributes to the spectrum other than the parameters of the top level which were used to train the ML model. Thus, all data points in Fig. 3 should fall on a line of slope 1 with vanishing residuals, i.e.,  $R^2=1$ . Consequently, slope and  $R^2$  directly measure how well each design suppresses the underlayer contributions.

The comparison of the test results for the four different target designs is shown in Fig. 4. Slope and  $R^2$  are plotted for the three test parameters of interest. For the conventional ML approach (blue), only the target with crossed lines suppresses the underlayer stack contributions as indicated by slope and  $R^2$  values close to 1 for all three parameters of interest. Noteworthy, a single crossed line pair comprising only two metal levels is sufficient to suppress all underlayer contributions. The parallel line scenarios with and without shift between the metal levels lead to similar poor results, confirming that the naïve notion of filling the gaps when viewing the structure from the top does not work for electromagnetic waves. For the VTS ML test (red), excellent slope and  $R^2$  values are achieved for each target design. This demonstrates that the VTS approach works well to suppress underlayer contributions independent of the target design choice.

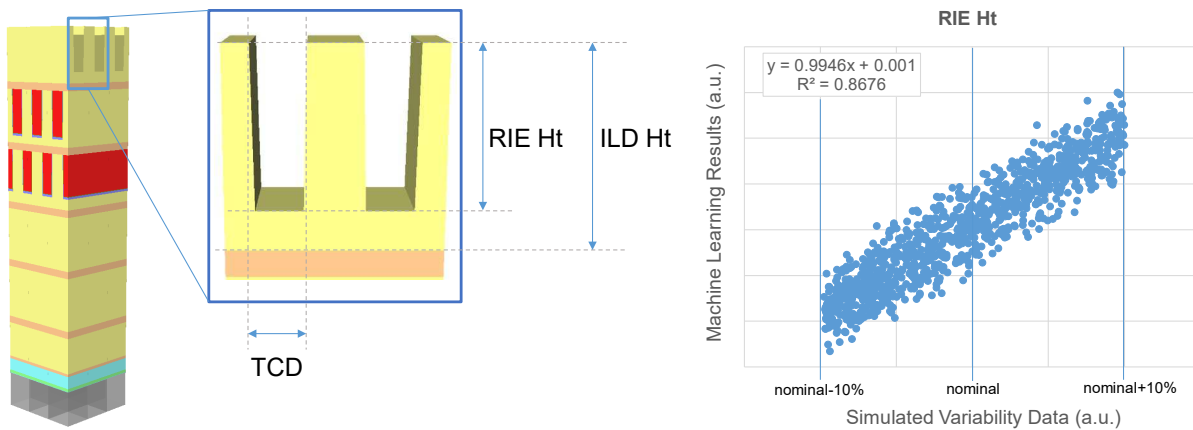


Figure 3. Parameters of interest for a post-RIE measurement step and respective data set when applying a ML model to simulated variability test data. The slope and  $R^2$  of a linear fit to the data set are a measure for how well a given target design suppresses underlayer contributions.

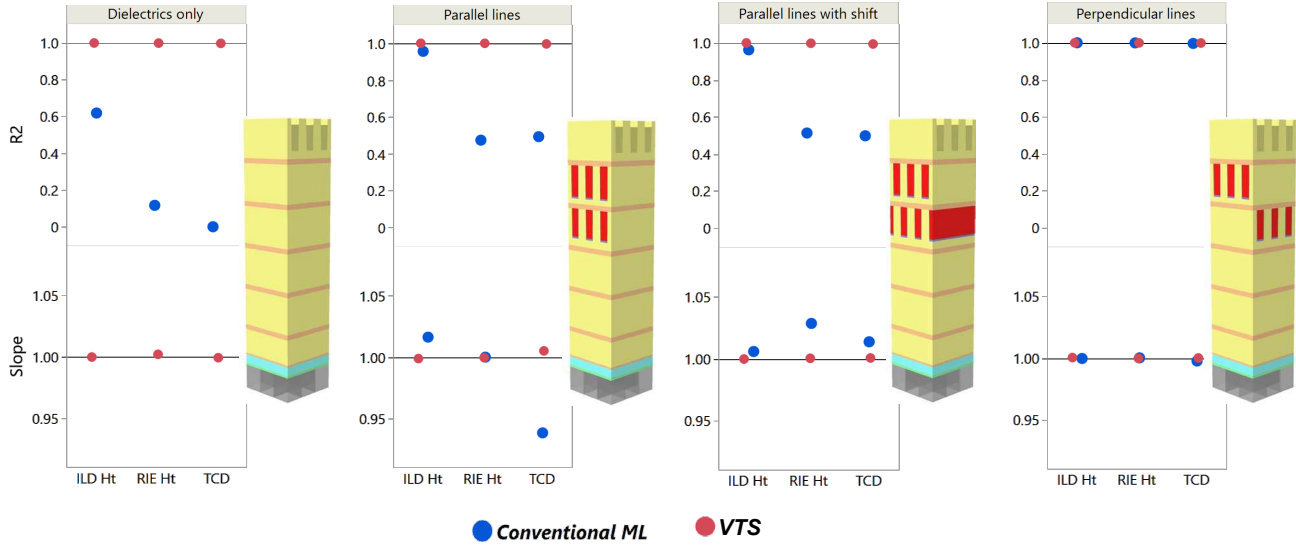


Figure 4. Results of the conventional ML (blue) and VTS ML (red) tests for the four proposed target designs. Slope and  $R^2$  results are shown for the three parameters of interest. Note, that the slope values for the conventional ML test in the dielectrics only case deviated so much from 1 that they fall outside the plotted range.

To assess the limitations of the single-crossed line pair approach, the difference of two stacks, one with nominal ILD height and another with double the ILD height in the first level, was evaluated for a wide range of half-pitches. Figure 5 shows the resulting merit function (MF) normalized by a typical threshold value for an acceptable match of an RCWA model to spectral data for the Nova Prism tool. A value below 1 indicates that the crossed-line approach suppressed the underlayer contribution, and a value above 1 indicates that a single line pair may not be sufficient. For a metal line height of 90 nm, the single crossed-line pair approach successfully suppresses the underlayer contributions over a wide range of half-pitches. Only at very large half-pitches, the single crossed-line pair approach fails. When considering typical single-expose EUV lithography half-pitches ( $< 40$  nm) but reducing the metal line height to more realistic values such as 40 nm, the single crossed-line pair approach also fails as the copper lines become partially transparent even for parallel polarization. In that case, either more than one pair of crossed lines needs to be present under the level of interest, or the VTS approach can be applied, again, independent of the actual target design.

## 4.2 Post-CMP measurements at consecutive metal levels

Another important measurement step in the BEOL is the post-CMP measurement of metal line parameters such as line height and CDs. Measurements at a 3<sup>rd</sup> and 4<sup>th</sup> metal level are considered for this example. The main goal was to establish an alternative approach to the ML-based test in the previous section to identify the ideal target design for underlayer suppression while also investigating the applicable parameter range for the respective approaches. A standard RCWA model for a 4<sup>th</sup> metal level measurement is applied to a 3<sup>rd</sup> metal level spectral reflectivity data set for a wide range of nominal CDs and metal line heights (Fig. 6a). Presumably, a good match between the 4<sup>th</sup> level model and the 3<sup>rd</sup> level data is only achievable if the two levels beneath the top level of interest suppress all contributions from any levels beneath. In that case, the 4<sup>th</sup> level model would have the same spectral response as the 3<sup>rd</sup> level model.

A large set of randomized variability data was created again by varying all model parameters of a 3<sup>rd</sup> metal level RCWA model by up to 10% from the nominal values for a wide range of nominal metal line CDs and three typical metal-line-to-ILD- height ratios. A fixed pitch of 80 nm was assumed for all simulations. A 4<sup>th</sup> metal level RCWA model was then used

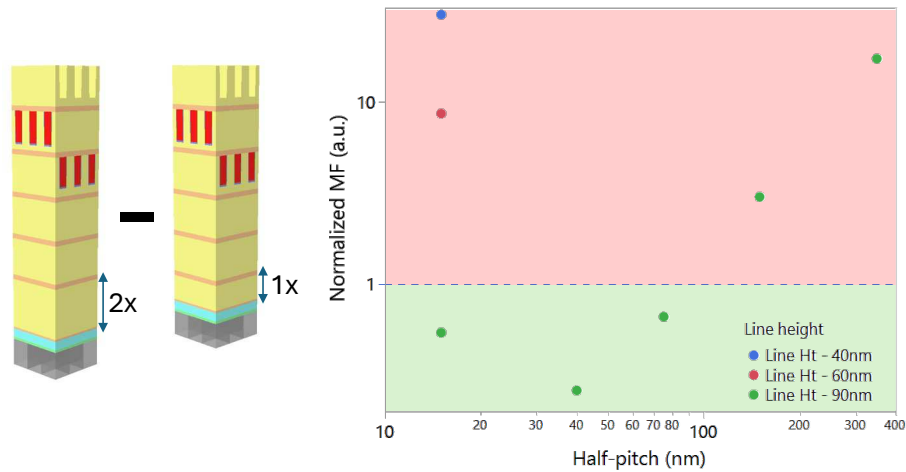


Figure 5. Merit function between models with nominal first level ILD height and doubled first level ILD height, normalized by a threshold value for an acceptable match of an RCWA model to spectral data for wide range of pitches and 3 different metal line heights. A value below 1 indicates a single pair of crossed lines suppresses underlayer contributions successful, above 1, the approach will likely fail to suppress all underlayer contributions.

to match the variability data. A parallel line design and a crossed line design were compared. Figure 6(b) shows a typical data set that is retrieved from the data analysis. Each data point represents the result after a regression analysis when applying the 4<sup>th</sup> metal level RCWA model to the 3<sup>rd</sup> metal level variability data set. The x-axis represents the known parameter value for each data set simulated by using the 3<sup>rd</sup> metal level RCWA model, the y-axis is the reported parameter value when applying the 4<sup>th</sup> metal level RCWA model to the 3<sup>rd</sup> metal level data. Like the ML cases discussed above, the slope and R<sup>2</sup> for a linear fit to all data points are indicators how well the “blocking levels” suppress the underlayer contributions for each of the two target designs. In addition, a goodness-of-fit (GOF) parameter is reported for each data point and the average GOF for all data points can be utilized as another metric to evaluate the match between the RCWA model and spectral reflectivity data. A GOF close to 1 indicates that the 4<sup>th</sup> metal level RCWA model can match the 3<sup>rd</sup> metal level data well, despite the presence of another level underneath, indicating that the 3<sup>rd</sup> and 2<sup>nd</sup> metal lines suppress any contribution from the 1<sup>st</sup> level.

The results for the comparison between the crossed and parallel metal line designs are shown in Fig. 7. The normalized GOF (NGOF) and R<sup>2</sup> for the metal height parameter and top CD parameter in the level of interest are shown for a wide range of nominal metal line top CDs and three different metal-line-to-ILD-height ratios of the “blocking levels”. As expected, for the design with parallel metal lines under the level of interest (red), a good match of the 4<sup>th</sup> metal level

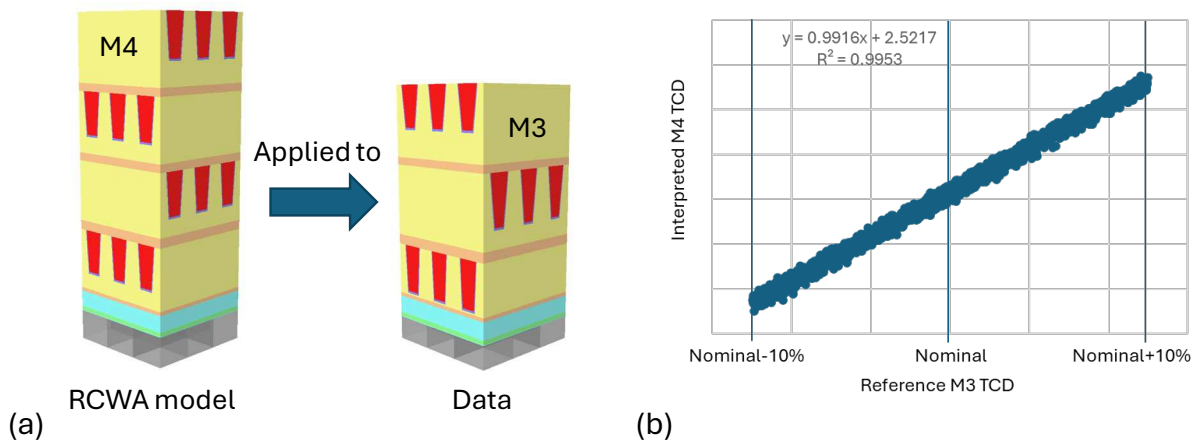


Figure 6. (a) Illustration of the application of a 4<sup>th</sup> metal level RCWA model to a 3<sup>rd</sup> metal level data set. (b) Representative data set showing interpretation results when applying a 4<sup>th</sup> metal level RCWA model to spectral reflectivity data simulated by varying all parameters of a 3<sup>rd</sup> level RCWA model by up to 10% around their nominal values.

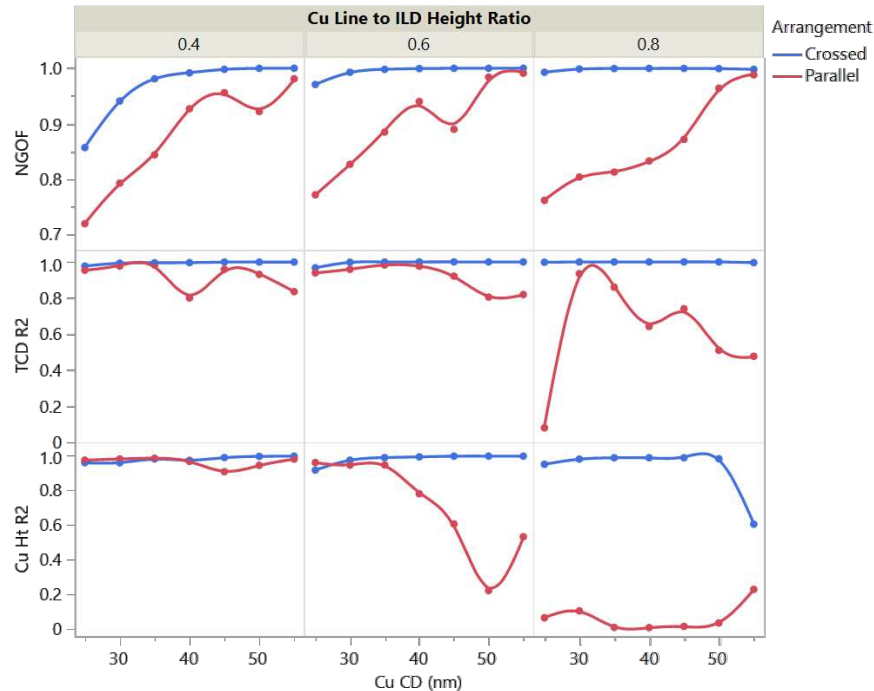


Figure 7. Resulting NGOF and  $R^2$  for Cu line height and line top CD in the level of interest when applying a 4<sup>th</sup> metal level post-CMP RCWA model with crossed metal lines under the top level (blue) and parallel metal lines under the top level (red) to simulated 3<sup>rd</sup> metal level data. Results are shown for a wide range of nominal metal line CDs and three different metal-line-to-ILD-height ratios. A metal line pitch of 80 nm was used for all simulations.

RCWA model to the 3<sup>rd</sup> level data was not achieved for either metal-line-to-ILD-height ratio independent of the nominal line CD. Only for very large nominal line CDs where the lines nearly resemble solid metal pads under the level of interest, acceptable GOF values are obtained. However, even in that case, the  $R^2$  for metal line height and top CD deviate significantly from 1 indicating that some contributions from the 1<sup>st</sup> level are still part of the 4<sup>th</sup> level model response when applied to the 3<sup>rd</sup> level data. In contrast, for the design with crossed metal lines under the level of interest (blue), excellent NGOF and  $R^2$  values are observed for most nominal line CDs and each of the metal-line-to-ILD-height ratios. This illustrates that the crossed line design successfully suppresses underlayer contributions and is applicable for wide range of line CDs and metal-line-to-ILD-height ratios.

For this example, experimental data was available to test the concept on production data. Polarized spectral reflectometry data at normal and oblique angles and for several azimuth angles was obtained on scribe line targets on a BEOL short loop wafer with crossed metal lines in each metal level. Data was acquired after the third metal level CMP step and the fourth metal level CMP step. First, an RCWA model was developed for measurements after the 4<sup>th</sup> metal level CMP step. The resulting match of the model to the experimental data is shown in Fig. 8 (top). An excellent GOF of 0.9951 was achieved. As expected, only parameters in the 2<sup>nd</sup>, 3<sup>rd</sup>, and 4<sup>th</sup> level showed any spectral sensitivity while the parameters of the first level could be fixed at arbitrary values. The same model was then applied to the experimental data from the measurement post-CMP at the third metal level. The only adjustment necessary was to rotate the polarization directions assigned in the experimental data by 90° to account for the different orientation of the metal lines at the 3<sup>rd</sup> metal CMP step compared to the 4<sup>th</sup> metal level. Figure 8 (bottom) shows the results when regressing the 4<sup>th</sup> metal level model to the 3<sup>rd</sup> metal level data without any further modification in the model structure. Note the change in color between the experimental data (lines) and model data (dots) due to rotation of the polarization direction in the experimental data. The excellent GOF of 0.9958 indicates that the 4<sup>th</sup> metal level model can match the 3<sup>rd</sup> metal level data very well. This demonstrates that a single model with crossed metal lines under the level of interest can be applied to several metal level post-CMP measurements without the need for model redevelopment if targets with respective crossed line are available and the pitch of the level of interest is the same between the different metal levels and similar processing is used.

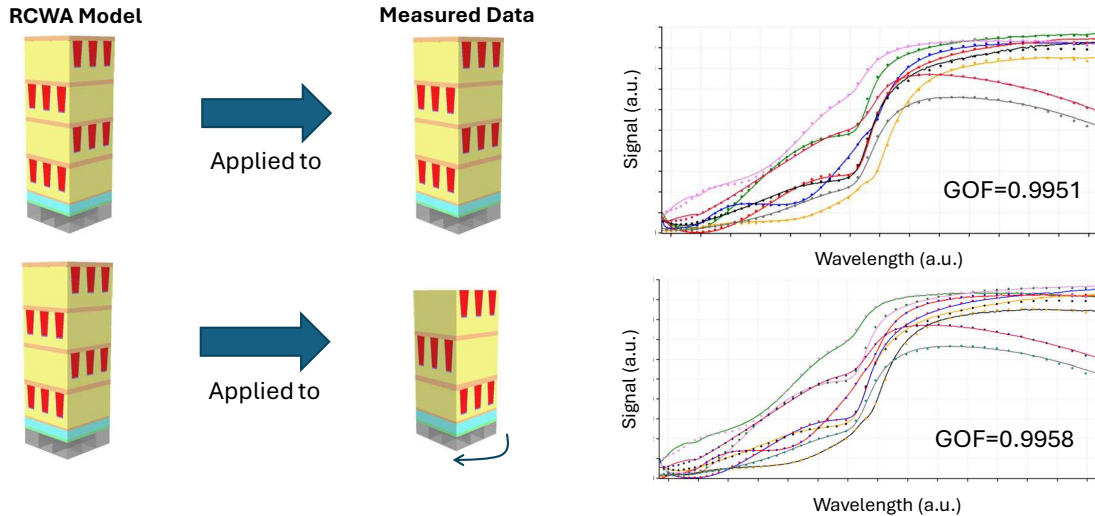


Figure 8. Model to experimental data match when applying a 4<sup>th</sup> level RCWA model to measured polarized spectral reflectometry data after the 4<sup>th</sup> metal level CMP step (top) and when applying the same model without modifications to polarized spectral reflectometry data acquired after the 3<sup>rd</sup> metal level CMP step (bottom). Note the change in colors between the experimental data (lines) and model data (dots) due to a 90° rotation that was applied to the polarization direction in the 3<sup>rd</sup> metal level experimental data to account for the different orientation of the metal lines between the 4<sup>th</sup> and 3<sup>rd</sup> metal level.

### 4.3 Measurement of the ILD thickness above patterned metal lines

The measurement of an ILD thickness for a higher metal level can be challenging for various reasons. Often, measurement of the ILD thickness on fully integrated wafers is the only option in a production environment. Building an RCWA model for a fully integrated wafer is possible but may take a long time and can be cumbersome, for example when combining levels of different pitches and dimensions into one RCWA model. Setting up an RCWA model for a simple target with no metal patterning or only a single patterned metal level is much easier and faster. The simple target can either be a dedicated target on the same wafer or a short loop wafer with skipped patterning steps. A ML model can easily be trained on the

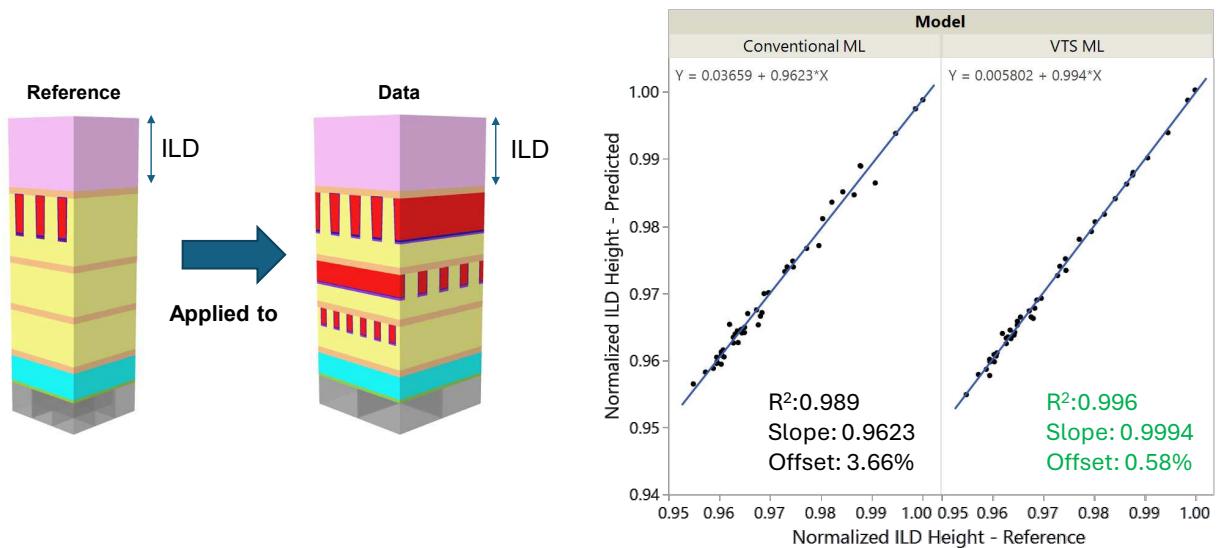


Figure 9. Results for the ILD height on a complex target when applying a ML model trained with reference data from a simple target in dependence on to the ILD height obtained by RCWA data analysis on a simple target on the same die and wafer. Conventional ML model results for measurements of polarized reflectivity data are compared to VTS ML model results with optimized filter position to remove underlayer contributions.

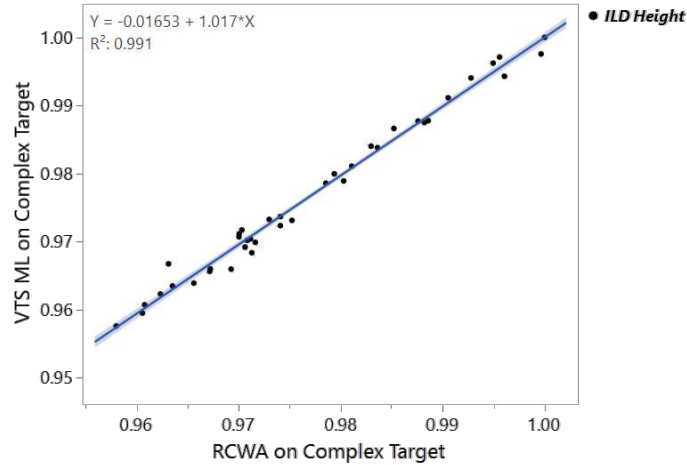


Figure 10. Comparison of the VTS ML results with conventional RCWA results obtained on complex target data.

simple target data with reference values for the ILD height as obtained from the RCWA model. When applying a conventional ML model trained on polarized spectral reflectometry data, variations in the underlayer structure might reduce the accuracy of the reported ILD height. Training the ML model on VTS data with optimized cut-off can reduce the contribution of the underlayer stack, and better accuracy is expected.

A comparison of results for a conventional ML model and a VTS machine learning model trained with reference data from a simple target and applied to a more complex target are shown in Fig. 9. The ML models were trained using a RCWA results from a simple target and assuming the same ILD thickness on a complex target on the same die. The training was done on one wafer, and two wafers (including the training wafer) were used for testing. The predicted ILD height on the complex target is shown in dependence of the measured ILD height using the RCWA model on the simple target on the same die and wafer. The conventional ML model predictions match the reference values well as indicated by very good  $R^2$ , slope, and offset parameter values. Note that underlayer contributions are suppressed by design as the two levels under the ILD layer are crossed metal lines. Nonetheless, when applying the ML model trained on VTS data with optimized filter position, an even better match to reference is achieved as indicated by excellent slope,  $R^2$ , and offset values, i.e., VTS improves the match to reference data compared to the conventional ML model by further reducing the influence of underlayer variability.

The VTS ML results were further validated by creating a full RCWA model for the complex target. The comparison of the VTS ML results with the conventional RCWA as measured on the same dies and wafer are shown in Fig. 10. Excellent match between the VTS ML results and RCWA results is evident from very good slope and  $R^2$  values. Compared to the RCWA analysis, the VTS ML approach provides much faster time to solution and easier setup.

## 5. SUMMARY AND CONCLUSIONS

BEOL metrology using scatterometry presents unique challenges due to the combination of different dimensions and complicated underlayer stacks. Target design opportunities and various metrology technique options can greatly simplify the analysis. A single pair of crossed metal lines is often sufficient to suppress underlayer contributions that otherwise would lead to parameter correlation and reduce the accuracy for the parameter of interest at the top level. The deliberate addition of crossed metal lines can significantly simplify RCWA models for ease of setup and fast turn-around times. A single model can be applied to several levels of comparable dimensions independent of the underlayer stack if crossed lines are present under the level of interest. VTS is universally applicable for BEOL metal level characterization independent of the target design choice. Simple targets may be used as a reference for ML models of complex targets. VTS ML provides superior performance over conventional ML even on optimized targets with crossed line underlayer suppression.

In conclusion, the co-optimization of target design and metrology techniques enables accurate measurement of critical dimensions of BEOL metal gratings for a wide range of dimensions, with reduced modeling effort and fast turnaround times.

### *Acknowledgements*

The authors would like to thank Asanka Weerasinghe, Claire Silvestre, Killian Chou, Luciana Meli, Paul Isbester, Jacob Ofek, and Smadar Ferber for fruitful discussions and support of this work.

## REFERENCES

- [1] Orji, N.G., Badaroglu, M., Barnes, B.M., Beitia, C., Bunday, B.D., Celano, U., Kline, R.J., Neisser, M., Obeng, Y. and Vladar, A.E., "Metrology for the next generation of semiconductor devices," *Nat. Electron.* 1, 532 (2018).
- [2] Breton, M.A., Schmidt, D., Greene, A., Frougier, J. and Felix, N., "Review of nanosheet metrology opportunities for technology readiness," *J. Micro/Nanopattern. Mats. Metro.* 21(2) 021206 (2022).
- [3] Timoney, P., Tsai, J., Baral, S., Economikos, L., Vaid, A., Lu, H., Kang, B., Isbester, P., Dasari, P., Kort, R. and Yellai, N., "Comprehensive BEOL control using scatterometry and APC," *Proc. SPIE* 9424, 94241G (2015).
- [4] Hafez, W., Agnihotri, P., Asoro, M., Aykol, M., Bains, B., Bambery, R., Bapna, M., Barik, A., Chatterjee, A., Chiu, P.C. and Chu, T., "Intel PowerVia Technology: Backside Power Delivery for High Density and High-Performance Computing," *2023 IEEE Symposium on VLSI Technology and Circuits (VLSI Technology and Circuits)*, pp. 1-2 (2023).
- [5] Timoney, P., Kagalwala, T., Reis, E., Lazkani, H., Hurley, J., Liu, H., Kang, C., Isbester, P., Yellai, N., Shifrin, M. and Etzioni, Y., "Implementation of machine learning for high-volume manufacturing metrology challenges," *Proc. SPIE* 10585, 105850X (2018).
- [6] I. Osherov, L. Issacharoff, O. Gedalia, K. Wakamoto, M. Sendelbach, M. Asano, "Application of advanced hybrid metrology method to nanoimprint lithography," *Proc. SPIE* 10145, 101451X (2017).
- [7] D. Schmidt, M. Medikonda, M. Rizzolo, C. Silvestre, J. Frougier, A. Greene, M. Breton, A. Cepler, J. Ofek, I. Kaplan, and R. Koret, "Spectral interferometry for fully integrated device metrology", *J. Micro/Nanopattern. Mats. Metro.* 22(3), 031203 (2023).
- [8] Yoon, J., Park, J., Shin, M., Ihm, D., Bismuth, O., Ferber, S., Ofek, J., Turovets, I. and Kim, I., "Unique spectral interferometry solutions for complex high aspect ratio 3D NAND structures". *Proc. SPIE* 12955, 129551S (2024).
- [9] D. Schmidt, C. Durfee, S. Pancharatnam, M. Medikonda, A. Greene, J. Frougier, A. Cepler, G. Belkin, D. Shafir, R. Koret, R. Shtainman, I. Turovets, and S. Wolfling, "OCD enhanced: implementation and validation of spectral interferometry for nanosheet inner spacer indentation," *Proc. SPIE* 11611, 116111U (2021).
- [10] Schoeche, S., Schmidt, D., Han, J., Butt, S., Sieg, K., Cheng, M., Cepler, A., Dror, S., Ofek, J., Osherov, I. and Turovets, I., "Spectral interferometry for TSV metrology in chiplet technology". *Proc. SPIE* 12955, 129551O (2024).
- [11] M. G. Moharam and T. K. Gaylord, "Diffraction analysis of dielectric surface-relief gratings," *J. Opt. Soc. Am.* 72, 1385 (1982).